

Magnetic field induced luminescence spectra in a quantum cascade laser

V. M. Apalkov and Tapash Chakraborty^{a)}

Max-Planck-Institut für Physik Komplexer Systeme, Dresden, Germany

(Received 7 September 2000; accepted for publication 29 January 2001)

We report on our study of the luminescence spectra of a quantum cascade laser in the presence of an external magnetic field tilted from the direction perpendicular to the electron plane. The effect of the tilted field is to allow novel optical transitions because of the coupling of intersubband-cyclotron energies. We find that by tuning the applied field, one can get optical transitions at different energies that are as sharp as the zero-field transitions. © 2001 American Institute of Physics.

[DOI: 10.1063/1.1359488]

The unipolar quantum cascade laser (QCL)¹ is the product of ingenious quantum engineering that exploits the properties of electrons confined in semiconductor nanostructures. As yet, this is the only high power semiconductor laser that operates at and above room temperature in the mid-infrared range.² The high power and tunability of QCL in the mid-infrared range have made the QCL an important device for gas-sensing applications.³ Here we propose a novel effect due to a tilted magnetic field on a QCL. An externally applied magnetic field that is tilted from the direction perpendicular to the electron plane provides two magnetic-field components: The parallel component of the field causes a shift in the energy dispersion in addition to a small diamagnetic shift.^{4,5} The perpendicular component, on the other hand, causes quantization of the subbands. Because of the shifts of the center of the Landau orbit in the wave-vector space, *combined intersubband-cyclotron transitions*, in addition to the usual intersubband transitions, are allowed.^{6,7} Our detailed calculations presented below indicate that as the subbands quantize into discrete Landau levels, new luminescence peaks appear that correspond to those new transitions. The peaks exhibit a prominent redshift but can be made as sharp and large as the zero-field case by tuning the applied field. The effect proposed here can be important for application because it shows that for a given QCL device, it is possible to shift the luminescence peak considerably by an external magnetic field.

The system we have studied here is sketched schematically in Fig. 1, where a GaInAs quantum well of 7.4 nm width is sandwiched between two AlInAs tunneling barriers. When a suitable bias is applied, electrons tunneling through the upstream barrier generate photons and escape quickly to the next well through the downstream barrier. Superlattice structures on both sides of the active region act as electron injector or Bragg mirrors and control the rate of electron escape.¹

An externally applied magnetic field tilted from the direction perpendicular to the electron plane is a well-studied problem experimentally as well as theoretically, in the con-

text of quantum Hall effects.⁶ For a magnetic field tilted from the z direction the perpendicular and parallel motions of electrons are coupled and as a result, transitions between different Landau levels of the ground and upper subbands become possible. The Hamiltonian of the system in a tilted field is

$$\mathcal{H} = \mathcal{H}_{\perp} + \mathcal{H}_{\parallel} + \mathcal{H}',$$

where

$$\mathcal{H}_{\perp} = \frac{1}{2m^*} p_z^2 + V_{\text{eff}}(z) + \frac{\hbar^2}{2m^*} \frac{z^2}{l_{\perp}^4},$$

$$\mathcal{H}_{\parallel} = \frac{1}{2m^*} \left[p_x^2 + \frac{\hbar^2}{l_{\perp}^4} (x+X)^2 \right],$$

$$\mathcal{H}' = \frac{\hbar}{m^*} \frac{z p_x}{l_{\parallel}^2},$$

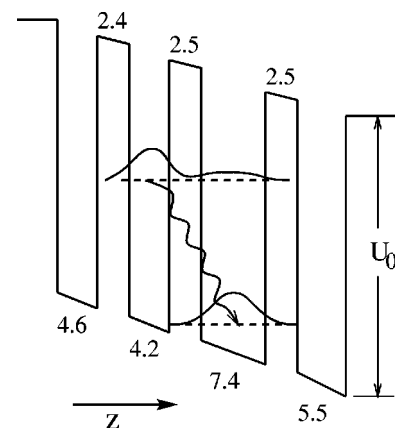


FIG. 1. Energy band diagram (schematic) of the active region of a quantum cascade laser structure under an average applied electric field of 55 kV/cm. Only one period of the device is shown here. The relevant wave functions (moduli squared) as well as the transition corresponding to the laser action are also shown schematically. The numbers (in nm) are the well ($\text{Ga}_{0.47}\text{In}_{0.53}\text{As}$) and barrier ($\text{Al}_{0.48}\text{In}_{0.52}\text{As}$) widths. Material parameters considered in this work are: electron effective mass m_e^* ($\text{Ga}_{0.47}\text{In}_{0.53}\text{As}$) = $0.043 m_0$, m_e^* ($\text{Al}_{0.48}\text{In}_{0.52}\text{As}$) = $0.078 m_0$, the conduction band discontinuity, $U_0 = 520$ meV, the nonparabolicity coefficient, $\gamma_w = 1.3 \times 10^{-18} \text{ m}^2$ for the well and $\gamma_b = 0.39 \times 10^{-18} \text{ m}^2$ for the barrier, and the sheet carrier density induced by doping, $n_s = 2.3 \times 10^{11} \text{ cm}^{-2}$. The energy difference between the two levels where the optical transition takes place, is 132 meV. All computations were performed at $T = 50$ K.

^{a)} Author to whom correspondence should be addressed; present address: Institute of Mathematical Science, Chennai 600113, India; electronic mail: tapash@mpipks-dresden.mpg.de

with $X \equiv (p_y/\hbar)l_{\perp}^2$ the center coordinate of the cyclotron motion and $l_{\parallel}^2 = c\hbar/eH_y$, $l_{\perp}^2 = c\hbar/eH_z$ are the magnetic lengths. Here we have chosen the Landau gauge vector potential, $\mathbf{A} = (H_y z, H_z x, 0)$. The magnetic field is therefore in the $y-z$ plane and $H_y = H \sin \theta$, $H_z = H \cos \theta$, where θ is the tilt angle, and H is the total magnetic field.⁶

The effective potential is made up of the (i) confinement potential, (ii) Hartree potential, and the (iii) exchange-correlation potential.⁸ The wave functions of the Hamiltonian \mathcal{H}_{\perp} , which depend only on the z coordinate, are obtained from

$$\mathcal{H}_{\perp} \psi_n = E_n \psi_n(z).$$

Solutions of this equation determine the energy levels and wave functions of the subbands. The total Hamiltonian is diagonalized by choosing the basis wave functions

$$\Psi_{n,N,X} = L^{-1/2} \exp\left(-i \frac{X}{y} l_{\perp}^2 - i \frac{z_{nm}}{l_{\parallel}^2} (x-X)\right) \times \xi_N(x-X) \psi_n(z),$$

$$\xi_N(x) = i^N (2^N N! \pi^{1/2} l_{\perp})^{-1/2} H_N\left(\frac{x}{l_{\perp}}\right) \exp\left(-\frac{x^2}{2l_{\perp}^2}\right),$$

$$z_{nm} = \int dz \psi_n(z) z \psi_m(z),$$

where $H_N(x)$ is the Hermite polynomial. The Hamiltonian matrix elements $\langle n'N'X' | \mathcal{H} | nNX \rangle$ are then calculated in this basis. The matrix is diagonal in X . To calculate the wave functions we use three subbands and 20 Landau levels on each subband.

Intensity of the optical emission is determined by the dipole matrix elements between initial (before emission) and final (after emission) states of the multielectron system. In dipole transitions the transition intensity is proportional to the overlap between (x,y) -dependent parts of the wave functions of the initial and final states. For a vanishing perpendicular magnetic field this results in conservation of the two-dimensional momentum in the optical transition. For nonzero perpendicular magnetic fields the states of the two-dimensional electrons are classified by two numbers: the Landau level index and by a number that distinguishes the degenerate states of an electron within a Landau level, for example, by the x component of the momentum. The energy of the single electron system depends only on the number of the Landau level, and the wave functions are harmonic oscillator functions whose center is determined by the x component of the momentum. If the magnetic field is directed perpendicular to the two-dimensional layer, then optical transitions are allowed only between the states with the same two-dimensional quantum numbers. In this case we will have a single line which corresponds to the optical transitions between states with the same Landau level index.

Introduction of a nonzero parallel magnetic field in the y direction results in modification of the wave function in a Landau level: the position of oscillator wave functions is now determined by the y component of the momentum and also by the average position of the electron in the z direction $\langle z \rangle$ that depends on the number of subbands. Figure 1 illustrates this dependence. Electrons in the first and second sub-

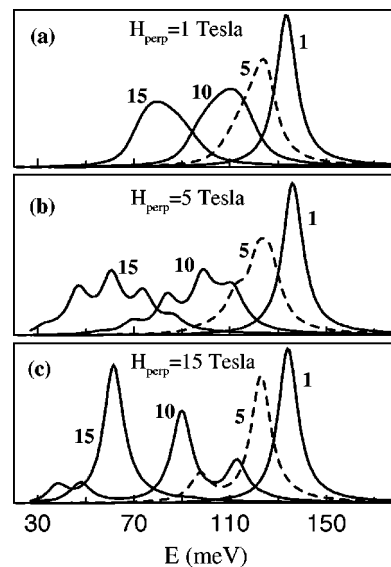


FIG. 2. Luminescence spectra at various values of the parallel component of the magnetic field, H_{par} (numbers by the curves in tesla) for: (a) $H_{\text{perp}} = 1$ T, (b) $H_{\text{perp}} = 5$ T, and (c) $H_{\text{perp}} = 15$ T.

bands are localized in the quantum wells 7.4 and 4.2 nm, respectively. This opens up the possibility for optical transitions between different Landau levels and at the same time it suppresses the optical transitions between the states with the same Landau level indices.

Evolution of the emission spectra as a function of the tilted magnetic field and tilt angle are illustrated in Figs. 2 and 3. In Fig. 2, the optical spectra are shown for three values of the perpendicular component of the field and for different values of the parallel component of the field for a fixed H_{perp} . Clearly, for small H_{perp} [Fig. 2(a)], the emission spectra do not feel the Landau quantization and we have a single peak that broadens with increasing H_{par} . For higher fields such as $H_{\text{perp}} = 5$ T [Fig. 2(b)], we find new features in the emission spectra. For a small parallel field, $H_{\text{par}} = 1$ T, main transitions are between the states with the same Landau

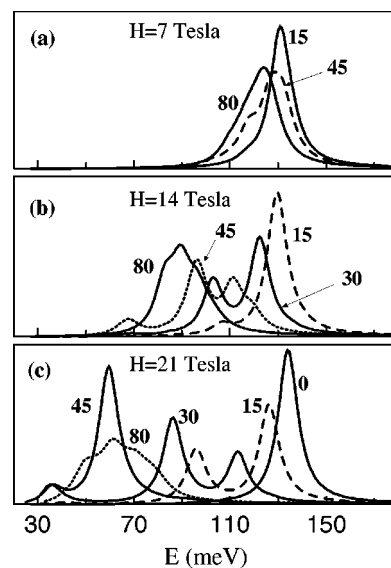


FIG. 3. Luminescence spectra at various values of the tilt angle (numbers by the curves) for the total magnetic fields: (a) $H = 7$ T, (b) $H = 14$ T, and (c) $H = 21$ T.

index, hence a single peak that corresponds to transitions from the zeroth Landau level of the second subband to that of the first subband. An increase of the parallel field makes transitions to higher Landau levels more intense. Appearance of a shoulder at $H_{\text{par}}=5$ T corresponds to transitions to the first Landau level of the first subband. Similarly, peaks at $H_{\text{par}}=10$ and 15 T correspond to transitions from zeroth Landau level of the second subband to the higher Landau level of the first subband. The energy separations between the peaks are equal to the separations between Landau levels of the first subband. In Fig. 2(c), transitions to the nonzero Landau level become more intense and we observe an interplay between the transitions to zero and to the first Landau levels with increasing parallel field. For a small H_{par} ($H_{\text{par}}=1$ T), there is only a strong transition to zeroth Landau level. For $H_{\text{par}}=5$ T, we observe the appearance of a small peak that corresponds to transitions to the first Landau level, and for $H_{\text{par}}=10$ and 15 T, transitions to the first Landau level become strongest and we observe the formation of a new narrow peak that corresponds to a transition to the first Landau level.

In Fig. 3, the emission spectra are shown for three values of the total magnetic field H and for different values of the tilt angle at a fixed H . For a small field [Fig. 3(a)] we have a redshift of the emission spectra with increasing parallel field (i.e., increasing tilt angle). For $\theta=45^\circ$ there is a weak structure resulting from the Landau quantization. At higher fields [Figs. 3(b) and 3(c)], one observes the evolution of the emission spectra from a broad peak at a large angle $\theta=80^\circ$ (large parallel field and a small perpendicular field) to a single narrow peak for small angle. In the latter case, the parallel component of the magnetic field is small and all optical transitions are transitions between the Landau levels with the same index. For an intermediate tilt angle, there are two peaks that correspond to transitions from the zeroth Landau level of the second subband to zeroth and the first Landau levels of the first subband. The intensity of transition to the first Landau level increases with increasing angle, which means an increase of the parallel field. It has its maximum at $\theta=45^\circ$ and

for total magnetic field of $H=21$ T one observes the formation of a strong narrow peak at $\theta=45^\circ$ associated with a suppression of the original peak corresponding to the transition to zeroth Landau level of the first subband. This is the same peak as shown in Fig. 2 for $H_{\text{perp}}=H_{\text{par}}=15$ T. It should be mentioned that our results are valid for impurity-free, or high-mobility electron systems, because in the presence of disorder due to interface roughness or due to charged impurities, the redshift of the emission line that is characteristic of the magnetic field effects⁴ tends to cancel out.^{9,5} From these results, we conclude that by suitably tuning the externally applied tilted field, lasing due to coupled intersubband-cyclotron transitions that is as strong as the zero-field case (but at different energies) can be achieved.

The authors would like to express their gratitude to P. Fulde for his kind support and for valuable discussions. They also thank S. Blaser for helpful discussions.

¹J. Faist, F. Capasso, D. L. Sivco, C. Sirtori, A. L. Hutchinson, and A. Y. Cho, *Science* **264**, 553 (1994); J. Faist, F. Capasso, C. Sirtori, D. L. Sivco, A. L. Hutchinson, and A. Y. Cho, *Appl. Phys. Lett.* **66**, 538 (1995).

²J. Faist, F. Capasso, D. L. Sivco, A. L. Hutchinson, S. G. Chu, and A. Y. Cho, *Appl. Phys. Lett.* **72**, 680 (1998); C. Gmachl, F. Capasso, A. Tredicucci, D. L. Sivco, A. L. Hutchinson, and A. Y. Cho, *Electron. Lett.* **34**, 1103 (1998); J. Faist, F. Capasso, C. Sirtori, D. L. Sivco, J. N. Baillargeon, A. L. Hutchinson, and A. Y. Cho, *Appl. Phys. Lett.* **68**, 3680 (1996); J. Faist, C. Sirtori, F. Capasso, D. L. Sivco, J. N. Baillargeon, A. L. Hutchinson, and A. Y. Cho, *IEEE Photonics Technol. Lett.* **10**, 1100 (1998); C. Sirtori, P. Kruck, S. Barbieri, P. Collot, J. Nagle, M. Beck, J. Faist, and U. Oesterle, *Appl. Phys. Lett.* **73**, 3486 (1998); P. T. Keightley, L. R. Wilson, J. W. Cockburn, M. S. Skolnick, J. C. Clark, R. Grey, G. Hill, and M. Hopkinson, *Physica E (Amsterdam)* **7**, 8 (2000).

³F. Capasso, C. Gmachl, A. Tredicucci, A. L. Hutchinson, D. L. Sivco, and A. Y. Cho, *Opt. Photonics News* **10**, 31 (1999).

⁴W. Beinvogl, A. Kamgar, and J. F. Koch, *Phys. Rev. B* **14**, 4274 (1976).

⁵V. M. Apalkov and T. Chakraborty, *Appl. Phys. Lett.* **78**, 697 (2001).

⁶T. Chakraborty and P. Pietiläinen, *The Quantum Hall Effects*, 2nd ed. (Springer, New York, 1995).

⁷T. Ando, *Phys. Rev. B* **19**, 2106 (1979).

⁸D. M. Ceperley and B. J. Alder, *Phys. Rev. Lett.* **45**, 566 (1980).

⁹S. Blaser, L. Diehl, M. Beck, and J. Faist, *Physica E (Amsterdam)* **7**, 33 (2000).